The 5th European sCO_2 Conference for Energy Systems
March 14-16, 2023, Prague, Czech Republic

2023-sCO2.eu-114

SYSTEM ANALYSIS OF EXPERIMENTAL SCO_2 CYCLE SOFIA

Daniel Kriz*
Research Centre Rez
Husinec-Rez, Czech Republic
Email: daniel.kriz@cvrez.cz

Petr Vlcek
Research Centre Rez
Husinec-Rez, Czech Republic

Otakar Frybort
Research Centre Rez
Husinec-Rez, Czech Republic

ABSTRACT

This work describes the one-dimensional, thermo-hydraulic model of the sCO_2 cycle Sofia which was made within the Efekt project to investigate optimal control methods and behaviour of the cycle during its operation. This dynamic model contains all devices like turbomachinery, heat exchangers or valves and piping including heat loss, according to the concept of the 1 MWe sCO_2 cycle, to be realised in the site of a fossil power plant in the Czech Republic.

Model assembly and calculations are performed with the commercial Modelica-based library ClaRaPlus using the simulation environment Dymola and in combination with another Modelica-based library, UserInteraction; the real-time simulations, with some parameter changes during the calculation, are made and described in this paper.

Nominal parameters were achieved during the steady-state simulation, except the lower mass flow of sCO_2. Transient simulation of power turbine start-up from standby state and results are also presented in this paper. The nominal state is achieved with the semi-automatic procedure in approx. 3 hours. The simulation results allow more detailed analyses of control methods and a better understanding of real device control and behaviour during start-up, shutdown, or other transients.

Careful manipulation with turbine valves in cooperation with the pressuriser operation was identified as crucial for optimal control of the system. Also, the initial amount of CO_2 in the pressuriser affects its behaviour during transients.

INTRODUCTION

Supercritical (sCO_2) cycles promise high thermodynamic efficiency and thus more effective use of the primary sources of energy. Moreover, the compactness of sCO_2 cycles and the possibility of combining these cycles with renewable sources of energy could support the decentralisation of the energy industry. However, these sources of energy are unstable, and it is necessary to balance the fluctuations of power production. From the point of view of the thermal cycles, this creates a requirement for relatively quick reactions of the entire system and its control, safety, and reliability.

The Efekt project supported by the Technology Agency of the Czech Republic is being performed in CVR. The main goal of this project is the development of effective means of bulk energy storage using a sCO_2 cycle to convert stored thermal energy to electricity and validation of the key components or control methods of this system. The turbomachinery, such as the power turbine or the starter and main compressors, were identified as the key components to be tested on a simple recuperative sCO_2 power cycle called Sofia that enables testing of turbines with power up to 1.8 MWe.

The construction of effective and reliable turbomachines, as well as research of capable control strategies for the systems, are significant obstacles to the commercial use of the sCO_2 cycles from the technical point of view. Therefore, the experimental cycle Sofia is being performed within the Efekt project.

For a better understanding of the cycle behaviour, a one-dimensional, thermo-hydraulic model of the Sofia cycle has been prepared. The modelling approach is quite detailed and considers several features like real turbomachines characteristics, including the inertia of the rotors. Also considered are printed circuit heat exchangers (PCHE) and brazed plate heat exchangers (BPHE) with advanced heat transfer models or heat capacity of components structure, including piping.

The thermo-hydraulic model enables verification of proposed strategies for the cycle control, or its behaviour, during both normal operation and transient states. This paper describes the main components of the Sofia cycle, including the modelling approach. Furthermore, a control system proposal for the whole cycle and electric heater will be presented. The last part of this

* corresponding author

DOI: 10.17185/duepublico/77271

paper presents selected results of the simulations, focused on the nominal steady state of the cycle and the power turbine start-up.

FACILITY PARAMETERS AND LAYOUT

The Sofia facility is a recuperative Brayton cycle with a compander – the main compressor driven by its radial turbine and the power turbine. The chosen design temperature of 565 °C is a compromise of the maximum working parameters of the modern supercritical Rankine steam cycles (600 – 700 °C) and acceptable investment costs. Operational parameters of 550 °C and 25 MPa were selected, as these parameters are considered suitable even for the energy use of sCO2 cycles. (Frýbort *et al.*, 2021)

The main modelled devices of the cycle are:

- Heat Supply – Electric Heater (6 MWe)
- Recuperative Heat Exchanger
- Water Cooler
- Pressuriser
- Radial Starter Compressor
- Compander – Main Radial Compressor, mechanically connected to the Radial Turbine
- Axial Power Turbine (1 MWe)

MODELLING PIPING AND FITTINGS

These main components are connected by pipes, as shown in Figure 1. The piping, including valves, is modelled with respect to the conceptual topology and dimensions of the real cycle. The model allows calculations of the local and friction losses, as well as heat losses and heat accumulation, to the piping walls.

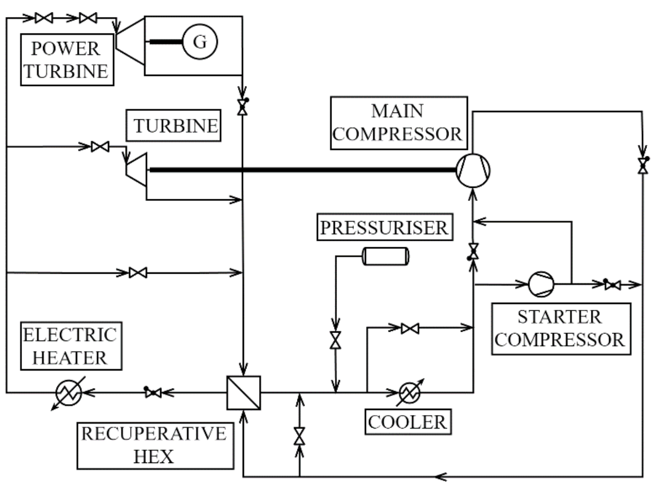

Figure 1: PFD scheme of the Sofia cycle model.

The ClaRa+ library from Dymola contains all the components needed for the pipes and fittings. The whole pipe model assembly in the Dymola environment is shown in Figure 2. One can see two walls in this figure. The first wall represents the steel wall of the pipe; the second wall represents thermal insulation. External heat losses are represented by a convective boundary condition. The pipeline modelling is important from the standpoint of determining the amount of CO_2 that will fill the facility.

Integral parts of the piping are fittings like control, closing or check valves. For testing the control strategies, it is necessary to include the exact design solution of the given fittings, represented in this case by the volume and closing speed of the valve. For these purposes, the components *GenericValveVLE_L1* and *ControlValveVLE_L1* from the ClaRa+ library were used. These models enabled the use of characteristics of the real valves, which were obtained from the manufacturer.

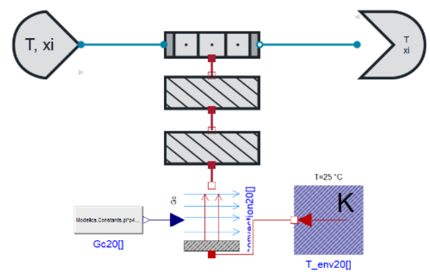

Figure 2: Pipe model assembly in Dymola. (XRG Simulation GmbH, 2022)

HEAT EXCHANGERS

Heat exchangers are probably the biggest challenge from the modelling point of view. The four heat transfer devices in the cycle all have different designs. Within the electric heater with the shell & tube design, there are electrical heating rods instead of tubes. The recuperative HEX is designed as a printed circuit heat exchanger (PCHE), see Figure 3. The cooler in Figure 4 is designed as a brazed plate heat exchanger (BPHE). Finally, the pressuriser is a shell & tube HEX with an electric heater, but with a combination of electric heating rods and water-cooled tubes. Thermo-hydraulic models of described heat exchangers have been developed in CVR using modified components from the ClaRa+ library.

The recuperative HEX is modelled as pure counter-current PCHE with semi-circular channels. Heat transfer and pressure drop are calculated only in these channels; distribution and collection parts of the HEX are neglected. The geometry is defined by the parameters according to Meshram *et al.* (2016) and described in Figure 3.

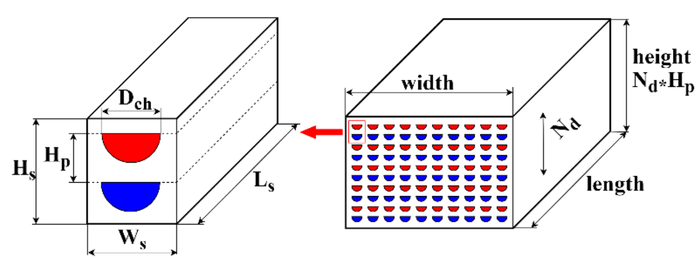

Figure 3: Description of PCHE. (Kriz, 2022)

Gnielinski equation is used for the turbulent flow convective heat transfer. It is

DOI: 10.17185/duepublico/77271

$$\mathrm{Nu} = \frac{(\xi/8)(\mathrm{Re} - 1000)\,\mathrm{Pr}}{1 + 12.7\sqrt{\xi/8}\,(\mathrm{Pr}^{2/3} - 1)}, \tag{1}$$

where ξ is the friction coefficient due to the modified equation

$$\xi = (1.82\log(\mathrm{Re}) - 1.64)^{-2}. \tag{2}$$

As shown in Table 1, heat transferred by recuperative HEX at nominal operation exceeds 8 MWt. Nevertheless, due to the microchannel design, the HEX is still relatively compact. Thermodynamic properties of supercritical CO_2 like low viscosity led to relatively low values of pressure drop. However, as mentioned before, distribution and collection parts of the HEX are neglected. Therefore, it is necessary to take the values of pressure drop given in Table 1 with a margin.

Table 1: Parameters of the recuperative HEX.

Parameter	Unit	LP	HP
Inlet temperature	°C	458	62
Outlet temperature	°C	101	313
Working pressure	MPa	8.40	25.40
Mass flow	kg/s	20.0	20.0
Pressure drop	kPa	59.91	19.96
Number of channels – one plate	-	201	201
Number of plates	-	66	66
Fluid volume	dm3	18.19	18.19
Avg. heat transfer coef.	W/m²K	3170	4120
Heat transfer area	m²	55.93	
Heat transferred	kW	8308	
HEX width	m	0.503	
HEX height	m	0.211	
HEX length	m	0.820	

Like the recuperative heat exchanger, the smallest possible dimensions are also desirable in the case of the cooler. However, river water is used as a coolant. In this case, the use of PCHE is not an ideal solution because of the higher risk of fouling and the probable higher pressure drop at the water side. Therefore, a brazed plate heat exchanger appears to be a better solution for this type of application.

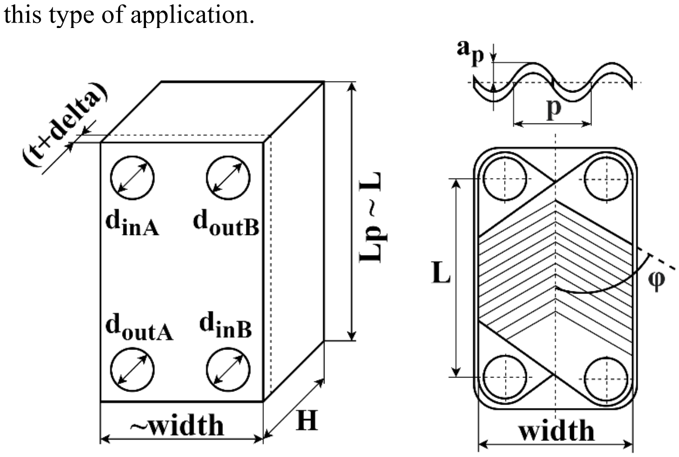

Figure 4: Description of BPHE. (Kriz, 2022)

The geometry of the model is shown in Figure 4. The parameters of the cooler are listed in Table 2. The modelling approach of the cooler is based on the methodology described in VDI (2010). Counter current flow is considered. Similar to the PCHE model, heat transfer and pressure drop are calculated only in the channels part. The value of this pressure drop is listed in Table 2.

Table 2: Parameters of the cooler.

Parameter	Unit	CO_2	Water
Inlet temperature	°C	100	16
Outlet temperature	°C	30	30
Working pressure	MPa	8.00	1.10
Mass flow	kg/s	20.0	81.0
Pressure drop	kPa	24.50	101.93
Number of plates	-	380	
Number of channels	-	189	190
Fill volume	dm3	128	18.19
Overall heat transfer coef.	W/m²K	2564	
Heat transfer area	m²	94.55	
Heat transferred	kW	4747	
Width	m	0.386	
H	m	0.878	
L	m	0.875	

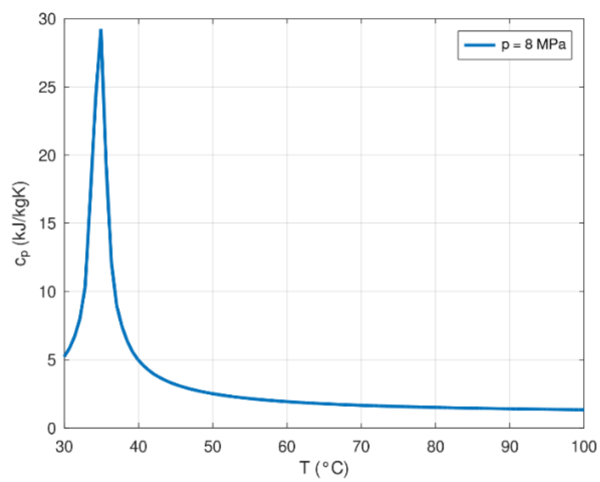

Figure 5: Isobaric heat capacity of CO_2 – temperature dependence.

Additional pressure drop in distribution and collection channels are estimated based on the similarity to flow in a circular tube. The heat transfer coefficient between plates is determined by the modified Lévêque basic equation according to VDI (2010).

$$\mathrm{Nu} = 1.615\left[\left(\frac{\xi\,\mathrm{Re}}{64}\right)\mathrm{Re}\,\mathrm{Pr}\,\frac{d_h}{L}\right]^{1/3} \tag{3}$$

and with the implementation of the Hagen number

DOI: 10.17185/duepublico/77271

$$2\mathrm{Hg} = \xi \mathrm{Re}^2 = \frac{\rho\, \Delta p\, d_h^3}{\mu^2\, L_p} \tag{4}$$

has the following form

$$\mathrm{Nu} = c_q\, \mathrm{Pr}^{1/3} \left(\frac{\mu}{\mu_w}\right)^{1/6} [2\mathrm{Hg} \sin(2\varphi)]^{1/3}. \tag{5}$$

In Table 2, it is also noticeable that the CO_2 temperature decreases below the critical temperature during cooling. This leads to a significant change in the thermodynamic parameters of the CO_2, especially isobaric heat capacity, as one can see in Figure 5. This phenomenon has a big influence on the temperature field in the cooler, and in some cases can cause problems with pinch point. (Dostál, 2005)

The electric heater is the largest device in the cycle. As mentioned before, it is a shell & tube type, but there are electric heating rods instead of tubes for the heating medium. Various numbers of heating rods are electrically joined to two heating segments with different sizes and power. There is a set of three heating U-rods called the heating cell. It has an output power of 30 kW (10 kW per heating rod). 27 heating U-rods are joined to the heating cluster, with 270 kW of output power.

The whole heating system is divided into three tubular vessels (TOH1, TOH2, TOH3). In each of the vessels, there are two bundles of 10 heating cells and three heating clusters, i.e., 111 electric heated U-rods in each bundle with an overall power of 1110 kW. With six bundles, TS1 – TS6, we have an electric heater with a power of 6660 kW. For modelling purposes, the U-rods were replaced by 222 straight rods. This simplified geometry can be seen in Figure 6.

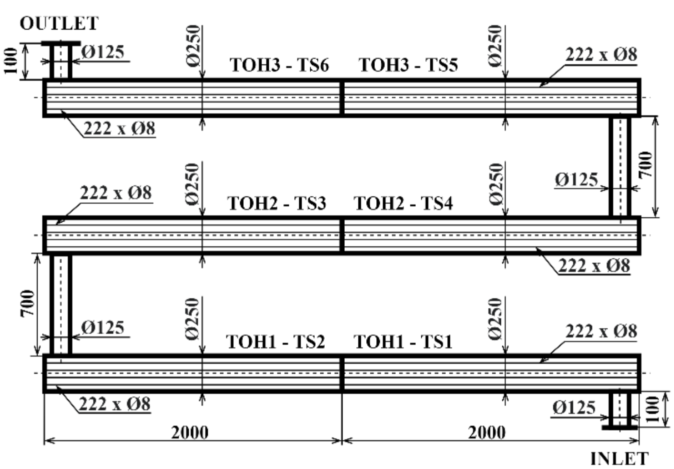

Figure 6: Simplified geometry of the electric heater.

Common semi-circular baffles for the shell & tube HEX are not used, and the longitudinal flow of CO_2 is considered. This approach promises to minimise the risk of the heating rods overheating due to a wake behind the semi-circular baffles. However, baffles cannot be completely omitted because they improve the stability of the heating rods. Therefore, perforated circular plates are used instead of standard baffles. In the thermo-hydraulic model of the electric heater, no baffles are considered. The pressure drop of the electric heater in several states is determined by CFD simulation, and this is implemented in the Modelica model as a nominal parameter that is used for recalculation of the pressure drop in any other state.

The heat transfer area of the electric heater depends on a number of active heating rods that change during its operation. Therefore, several standard ClaRa+ components were modified. The component *ShellFlowVarBundleVLE_L4* allows for calculations of heat transfer with temperature and pressure fields in the axial direction during longitudinal flow around a tube bundle. Even the amount of heat accumulated in a heating rod depends on its state. There is a larger amount of heat stored in active rods, with higher temperatures than in disabled rods. The mass of heating rods and the accumulation of heat in them is represented by modified component *CylindricalThinWall_L4*, where active and disabled rods are distinguished.

TURBOMACHINES

The turbomachinery, such as the power turbine, starter compressor, main compressor and its turbine were identified as the key components for the development and testing in the Sofia cycle. Development of these machines is challenging, especially from a technical point of view, due to their small size in combination with high performance. Before the Sofia cycle commissioning, it was necessary to perform some numerical studies.

Results from CFD or FEM simulations of a standalone turbomachinery or its parts can help with the optimisation of the geometry and mechanical durability. Other important outputs of the CFD simulations are the hydraulic and performance characteristics of turbomachines, which are used in the 1-D analysis of the whole cycle in Dymola.

With these simulations, it is possible to check the behaviour of turbomachines together with all the cycle devices, even during transient states. For these purposes, 1-D numerical models of a compressor and turbine were developed in CVR, based on ASME (1998) methodology and realised with Modelica code and ClaRa+ library. The model allows non-dimensional hydraulic and performance characteristics implementation. Therefore, it is possible to perform simulations in a wide range of parameters.

REGULATION AND CONTROL STRATEGIES

There are five main control loops in the Sofia facility. The first one is pressure control at the inlet of the main, or starter, compressor. This pressure is controlled by the pressuriser. The second control loop is temperature control at the inlet of the main, or starter, compressor, provided by the water cooler and its bypass. The pressure at the outlet of the main compressor is controlled by a valve at the compander turbine inlet, which also affects the speed of the whole compander, i.e., main compressor. This pressure can also be controlled with the valve in the bypass of the turbines, which is used in some operation states. The admission temperature of the turbines is provided by the electric

DOI: 10.17185/duepublico/77271

heater. The control system of this facility is extremely complex and will be partly described in the next paragraph. The last control loop is the output power control of the power turbine by a control valve at the power turbine inlet. However, this control loop was not yet used in simulations.

The electric heater described in the previous chapter has several heating elements with variable heating power. In every heating bundle, there are some proportional controlled and some two-position controlled heating cells (a set of three heating U-rods with a maximum power of 30 kW). Moreover, there are some two-position controlled heating clusters (a set of 27 U-rods with a maximum power of 270 kW). Each of the described heating segments is used for outlet temperature regulation. Activation of the specific heating segment depends on boundary conditions, like the mass flow of CO_2, and on the location of the previously activated heating segment. This approach will provide uniform heating of the filling in all the vessels of the heater. At the same time, the dependence on the mass flow reduces the risk of overheating certain parts of the electric heater.

THE CYCLE MODEL BENCHMARKS

All of the described sub-models of components and control loops form the overall model of the Sofia cycle. The first test of the model is a steady-state simulation of the nominal operation state that will prove interactions between individual components and the stability of the initialisation setup. It is also the first opportunity to see how the control loops react to small changes in controlled parameters. The results of the simulation were compared with design parameters, as shown in Table 3.

Table 3: Nominal parameters of Sofia facility.

	Inlet			Outlet	
	T °C	P MPa	m kg/s	T °C	p MPa
COMPRESSOR C.	30	8.00	20.0	62	25.50
RECUP HEX HP	62	25.47	20.0	312	25.32
EL. HEATER	312	25.26	20.0	550	25.16
TURBINE C.	550	25.06	6.5	448	8.50
POWER TURBINE	550	25.07	13.5	468	8.50
RECUP HEX LP	461	8.41	20.0	100	8.26
COOLER	100	8.23	20.0	30	8.19

From the following results of the steady-state simulation in Table 4, it can be seen, that the nominal mass flow was not reached. This was caused by the design characteristics of the turbomachines and their mutual interaction. According to the CFD characteristics, the compander turbine and power turbine are slightly more effective and need a lower mass flow and pressure ratio to achieve the required performance. This leads to compander turbine throttling and to a reduction of the overall mass flow in the cycle.

Table 4: Results of the steady-state simulation.

	Inlet			Outlet	
	T °C	p MPa	m kg/s	T °C	p MPa
COMPRESSOR C.	31	8.00	17.6	62	25.29
RECUP HEX HP	62	25.25	17.6	314	25.32
EL. HEATER	314	25.13	17.6	550	25.08
TURBINE C.	548	20.26	5.1	449	8.25
POWER TURBINE	550	24.98	12.5	460	8.36
RECUP HEX LP	457	8.24	17.6	99	8.14
COOLER	98	8.10	17.6	31	8.09

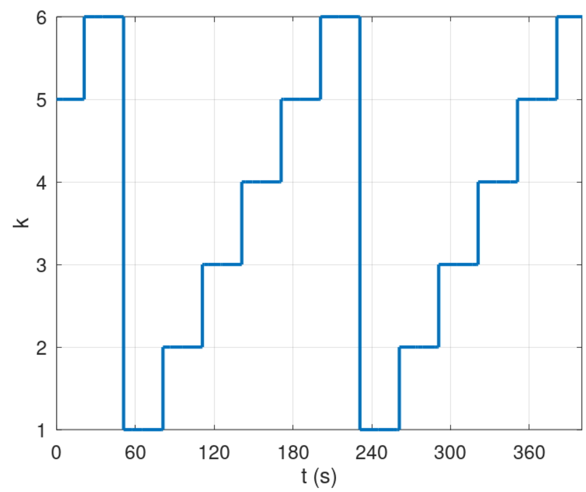

Figure 7: Sampling for heating segments control.

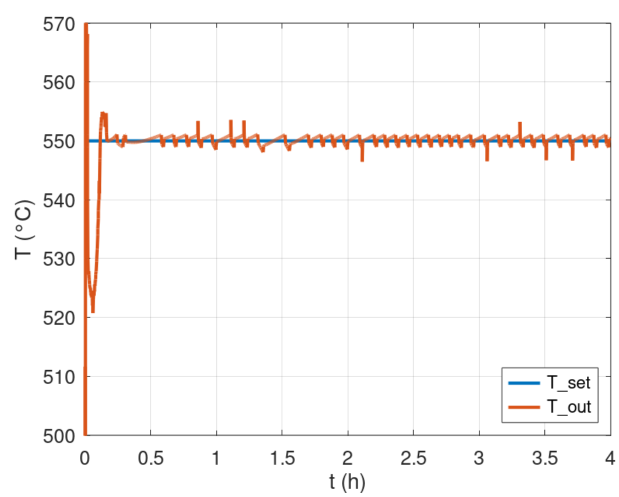

Figure 8: Nominal outlet temperature of the electric heater.

The electric heater output temperature can be seen in Figure 8. A large discontinuity at the beginning of the simulation was caused by initialisation. Only two-position control of the electric heater was active during this simulation. Therefore, the output temperature varied within certain limits. These limits were different for heating cells (± 1 °C offset) and for heating clusters (± 10 °C offset). The wider tolerance for heating clusters

DOI: 10.17185/duepublico/77271

prevented excessive oscillations. The heating segments were triggered at different times across bundles. This was provided by the control sequence, see Figure 7, where the *k* means activated bundle (TS1 – TS6). Each bundle regulated the output temperature for 30 seconds. Then it was replaced with the next bundle, according to sequence, to prevent local overheating. The rest of the time bundles held a constant power from the last activation.

As mentioned before, the pressure at the compressor inlet is controlled by the pressuriser. It is a tempered vessel filled with CO_2. If there is low pressure at the inlet of the main compressor, the pressuriser heats the fluid inside. A specific volume of the fluid will increase and cause the pressure to increase. Alternatively, if the pressure is too high, the fluid in the pressuriser will be cooled and cause the reverse effect. Too large pressure fluctuations do not occur during a normal operation, and temperature in the pressuriser changes minimally, as one can see in Figure 9.

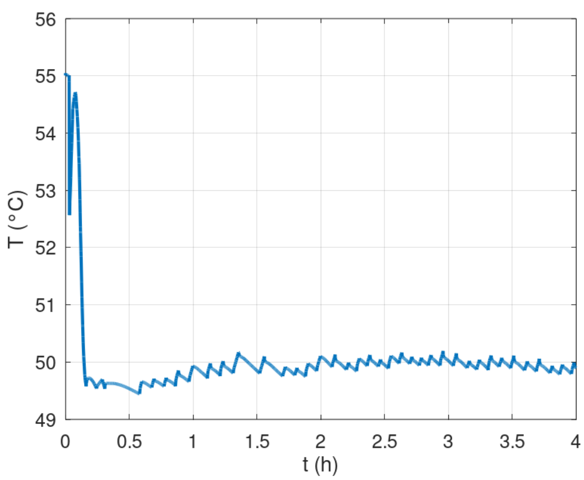

Figure 9: Temperature inside the pressuriser.

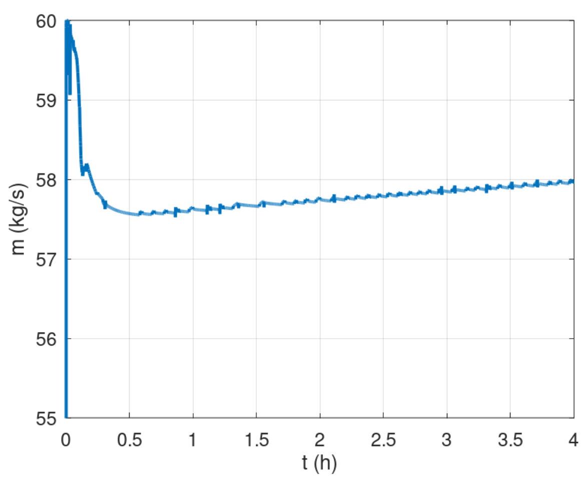

Figure 10: Water mass flow in the cooler.

In this case, the inlet temperature of the compressor was controlled by mass flow rate regulation of the cooling water, which is shown in Figure 10. It is also possible to control this temperature with a bypass of the Cooler for specific operation states. As one can see, the water mass flow is not completely steady, because the CO_2 output temperature from the cooler did not reach the setpoint of 30 °C yet. It has offset about 1 °C but changes slowly. Therefore, in this case, the state of the cycle can be evaluated as a steady state despite a slight increase in water mass flow.

According to the simulation, the power turbine produces about 1200 kW of output power during the nominal operation. The power consumption of the main compressor driven by its turbine ranges around 550 kW. The rotational speed of the whole compander is approx. 66,000 RPM.

RESULTS OF TRANSIENT SIMULATION

This thermohydraulic model is mainly created for research on the behaviour of the cycle during transient states, such as during start-up or shutdown. One of the tasks during the start-up procedure is the power turbine start-up. This can only be done if the compander turbomachinery works independently of the starter compressor and if there are some excess power and mass flow that can be used to drive the power turbine. This specific "standby" or "initial" state was determined by previous calculations and simulations. In this case, the power turbine start-up is provided by a semi-automatic control system. Some parameters are program-controlled, but several parameters, like valves opening or temperature setpoint, are controlled manually. This approach will most likely even be used for operating the real facility. In *Dymola*, the library *UserInteraction* is used for this type of operation. It allows the parameters of selected components to be changed during the simulation.

Parameters in the cycle in this standby state can be seen in Table 5. The main compressor must provide a sufficient mass flow for both the compander and the power turbine. It is obvious that if the power turbine is not operating, an excess mass flow rate must be diverted with a bypass. Therefore, the first operation during the power turbine start-up is a partial closure of the bypass valve and a partial opening of the valve at the inlet of the power turbine.

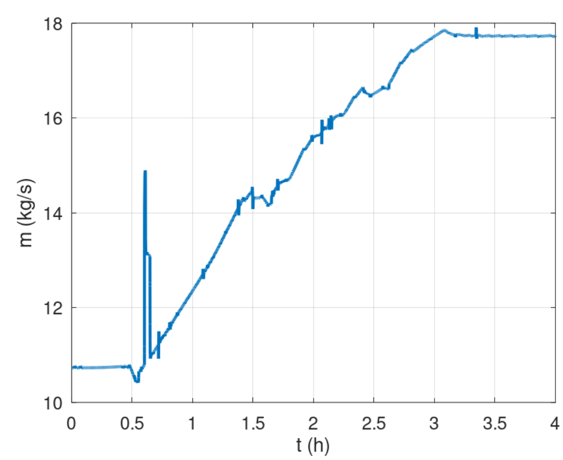

Figure 11: The overall mass flow rate development during the power turbine start-up.

DOI: 10.17185/duepublico/77271

In **Figure 11**, from 0.5–0.75 h, it can be seen, that the valve operations caused a temporary increase in the mass flow rate in the cycle. Valve cooperation, according to Figure 12, was not optimal; the power turbine valve opened a little bit faster and the pressure at the outlet of the main compressor decreased, but the power of its turbine was not changed. According to the main compressor characteristics, this leads to a higher mass flow rate.

Table 5: Standby (initial) state of the Sofia cycle.

	Inlet			Outlet	
	T °C	p MPa	m kg/s	T °C	p MPa
COMPRESSOR C.	28	8.02	10.9	40	14.51
RECUP HEX HP	40	14.49	10.9	161	14.48
EL. HEATER	161	14.45	10.9	300	14.38
TURBINE C.	296	13.02	3.8	257	8.11
POWER TURBINE	-	-	-	-	-
TURBS. BYPASS	298	14.36	7.1	286	8.11
RECUP HEX LP	276	8.10	10.9	55	8.07
COOLER	55	8.06	10.9	28	8.05

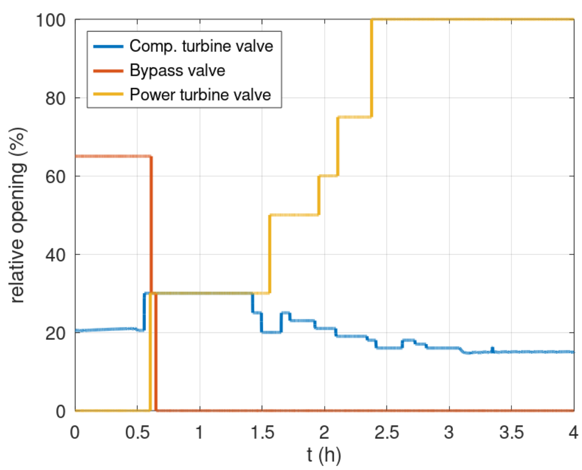

Figure 12: Relative opening of involved valves.

After this critical step, it is necessary to gradually reach the nominal parameters in the cycle. Increasing the outlet temperature from the electric heater in combination with manual control of the compander rotational speed using the compander turbine control valve proved to be a suitable way for reaching the nominal parameters. As one can see in Figure 13, a setpoint of the temperature was changed manually several times, and the electric heater control system automatically held the required value. According to the sampling in the electric heater control system, various heating segments are activated across the electric heater at different times. For example, Figure 14 shows how the power of two different heating segments (cell and cluster) in two different bundles is changing during the operation.

As the power of the compander increases, the opening of the valves may not always correspond (Figure 12), and there can be a lack of CO_2 in low-pressure parts of the cycle. This results in a decrease of pressure at the inlet of the main compressor, and it must be balanced by an increase in temperature in the pressuriser, see Figure 15. As the temperature increases, the specific volume of CO_2 also increases, which leads to an increase in pressure thus forcing the CO_2 out of the pressuriser to the Low-pressure side, as shown in Figure 16, which describes the development of the mass of CO_2 in the cycle during the start-up. The distribution of the volume and mass of CO_2 in the cycle is described in Table 6.

Table 6: Volume and mass of CO_2 in the cycle

		HP side	LP side	Pressuriser	Overall
Volume	dm^3	1000	887	659	2546
Mass - start	kg	218	194	110	522
Mass - end	kg	245	167	110	522

However, the pressuriser has limited possibilities to handle these fluctuations due to the maximum operating temperature of 130 °C and a power of 15 kW. Therefore, the operation of valves must be carefully done in concert with the temperature development in the pressuriser. This temperature, in context with pressure at the inlet of the main compressor, is shown in Figure 15.

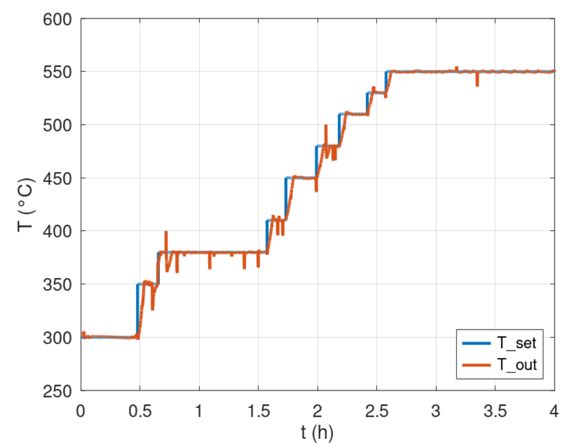

Figure 13: The electric heater outlet temperature development.

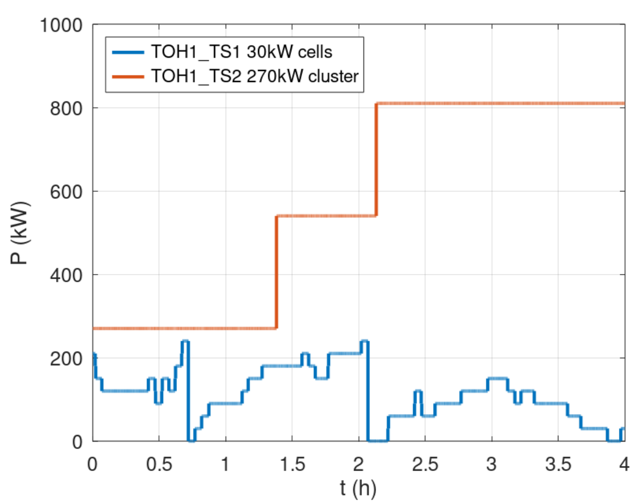

Figure 14: The power of selected heating segments.

DOI: 10.17185/duepublico/77271

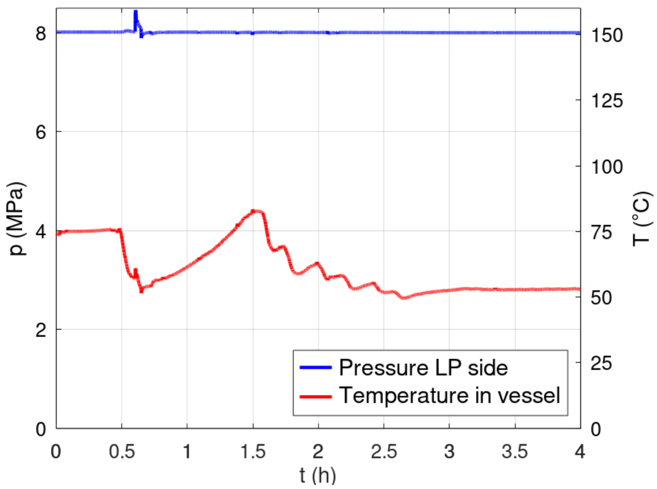

Figure 15: Temperature in the pressuriser and the pressure at the inlet of the main compressor.

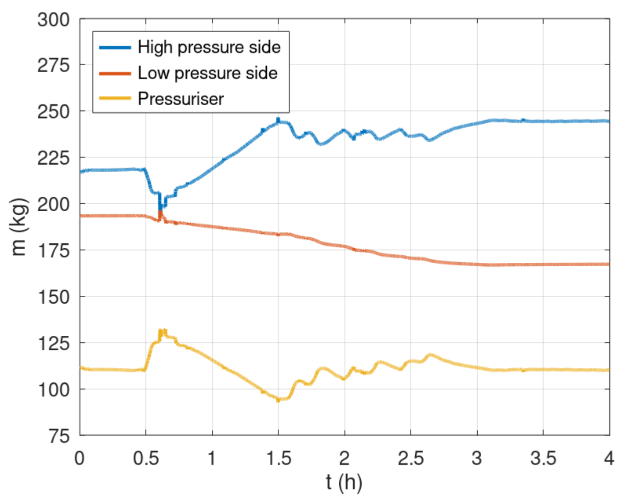

Figure 16: Mass of the CO_2 in the cycle

As in the previously described steady-state simulation, the inlet temperature of the main compressor was controlled automatically by regulation of the cooling water mass flow. Of course, more amount of CO_2 requires more amount of cooling water with a constant temperature. Therefore, increases during the simulation, as shown in Figure 17.

The increasing temperature in the system causes a specific volume change that leads to some pressure increase. At the same time, this pressure increase leads to the higher power of the compander, and this leads to another pressure and mass flow increase. Once again, increasing the temperature in the system was identified as the key part of the control. A throttling of the compander turbine requires only small interventions during this kind of start-up and is important mainly for the pressure balancing in low-pressure parts of the cycle. As shown in Figure 18, the main compressor outlet pressure increases by approx. constant gradient to the nominals.

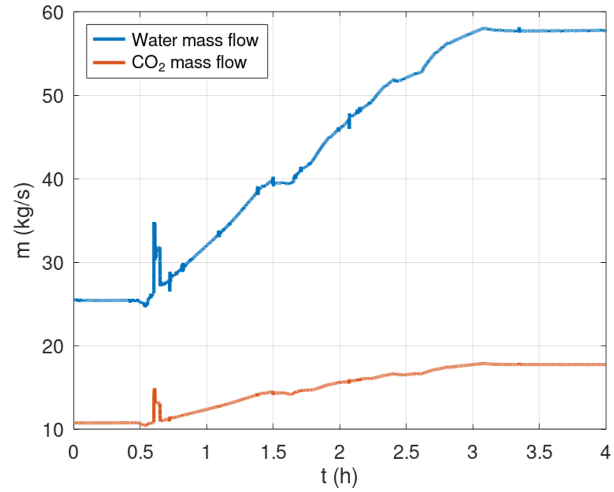

Figure 17: Cooling water and CO_2 mass flow.

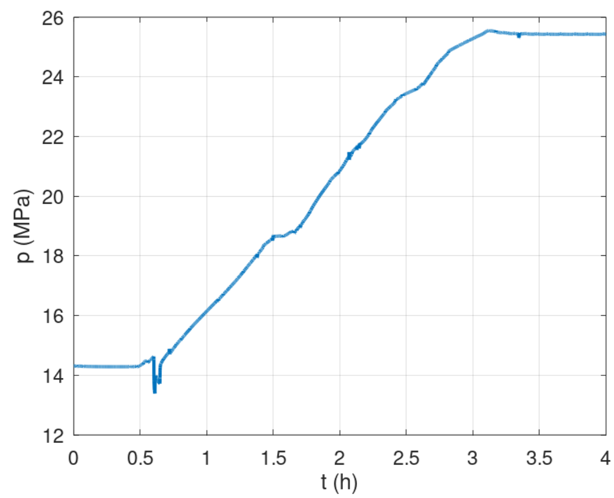

Figure 18: Main compressor outlet pressure.

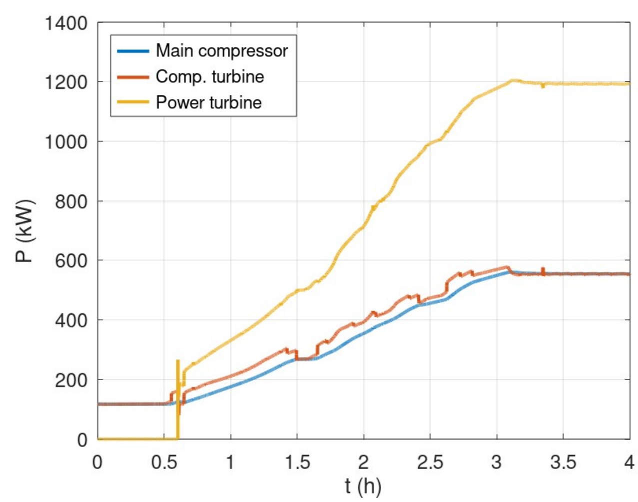

Figure 19: The power of turbomachines.

DOI: 10.17185/duepublico/77271

Finally, Figure 19 shows the power development of the turbomachines. The curves of the main compressor and its turbine overlap, according to mechanical connection. The power turbine started at zero power and gradually achieved the nominal power of approx. 1200 kW. During the whole simulated transient, the power turbine is in phase with the generator, and it has a constant, nominal rotational speed. As the admission pressure approached the nominal pressure, the automatic control of the compander turbine valve was triggered; from that moment, the cycle was controlled completely automatically.

CONCLUSION

Dymola software with ClaRa+ library, based on Modelica code, has been used in CVR for a long time; several numerical models created in it were experimentally verified at sCO_2 facilities by CVR or by its partners. This proves the usability of the mentioned software tools for these types of applications.

The results of the simulations can, therefore, be used with some certainty, even if the Sofia cycle is not yet in operation. The ability to test turbines with power up to 1.8 MWe enables the Sofia cycle to become the key facility for future commercial applications of the sCO_2 cycles. However, the determination of the optimal control strategies and the makeup of the main components are some of the more challenging issues.

For preliminary studies and systemic behaviour analyses of the Sofia cycle, the described 1-D thermo-hydraulic model was built within the Efekt project. All of the key components were created with respect to the concept designs of the real components. For example, complex models of the PCHE and BPHE heat exchangers were prepared, and non-dimensional turbomachines with characteristics determined by CFD simulations were used. Also, the control system of the electric heater, which is the largest facility in the Sofia cycle, was designed. Many steady-state and transient simulations were performed to support the development of the large-scale testing facility. Selected simulations - nominal steady state and power turbine start-up, were described in this paper to show the capabilities of the numeric model. Careful manipulation with turbine valves in cooperation with the pressuriser operation was identified as crucial for optimal control of the system. Also, the initial amount of CO_2 in the pressuriser affects its behaviour during transients. Work on the numerical model continues. There is still some room for optimisation, for example, a more detailed model of the power turbine and its equipment or control loops including delays, etc. However, the results of the performed simulations are already aiding the Sofia cycle realisation.

NOMENCLATURE

BPHE	Brazed Plate Heat Exchanger
C	Compander
c_q	Coefficient for Nusselt Number Calculation (-)
CVR	Research Centre Rez
Δp	Pressure Drop (kPa)
d_h	Hydraulic Diameter (m)
e	Electrical
φ	Wave Angle of Inclination (°)
HEX	Heat Exchanger
Hg	Hagen Number (-)
HP	High-Pressure Side
ξ	Friction Coefficient
L, Lp	Length of the Plate (m)
LP	Low-Pressure Side
μ	Dynamic Viscosity (Pas)
μ_w	Dynamic Viscosity at Wall (Pas)
Nu	Nusselt Number (-)
PCHE	Printed Circuit Heat Exchanger
Pr	Prandtl Number (-)
Re	Reynold Number (-)
ρ	Fluid Density ($kg.m^{-3}$)
sCO_2	Supercritical Carbon Dioxide
t	Thermal, Time (-, h)
TACR	Technology Agency of the Czech Republic

ACKNOWLEDGEMENTS

This work was supported by TACR THETA2, project no. TK02030059 (Efekt).

REFERENCES

[1] ASME (1998) ‘Performance Test Code on Compressors and Exhausters: An American National Standard’. New York: ASME.

[2] Dostál, V. (2005) ‘A supercritical carbon dioxide cycle for next generation nuclear reactors /’, 154.

[3] Frýbort, O. *et al.* (2021) ‘Sofia – sCO2 facility for supercritical Brayton cycle research’, *4th European sCO2 Conference for Energy Systems: March 23-24, 2021, Online Conference*. Edited by D. Brillert, pp. 185–193. Available at: https://doi.org/10.17185/duepublico/73942.

[4] Kriz, D. (2022) *Thermodynamic cycles working in supercritical region*. Czech Technical University in Prague.

[5] Meshram, A. *et al.* (2016) ‘Modeling and analysis of a printed circuit heat exchanger for supercritical CO2 power cycle applications’, *Applied Thermal Engineering*, 109, pp. 861–870. Available at: https://doi.org/10.1016/J.APPLTHERMALENG.2016.05.033.

[6] VDI (2010) *VDI Heat Atlas*. Berlin, Heidelberg: Springer Berlin Heidelberg. Available at: https://doi.org/10.1007/978-3-540-77877-6.

[7] XRG Simulation GmbH (2022) ‘ClaRaPlus’. Hamburg: XRG Simulation GmbH.

DOI: 10.17185/duepublico/77271

DOI: 10.17185/duepublico/77271
URN: urn:nbn:de:hbz:465-20230427-110440-9